Annals of Nuclear Medicine Vol. 21, No. 1, 25–32, 2007

Scatter correction based on an artificial neural network for ^{99m}Tc and ^{123}I dual-isotope SPECT in myocardial and brain imaging

Jingming BAI,* Jun HASHIMOTO,** Koichi OGAWA,*** Tadaki NAKAHARA,**
Takayuki SUZUKI** and Atsushi KUBO**

*21st Century Center of Excellence Program, **Department of Radiology, School of Medicine, Keio University
***Department of Electrical Informatics, Faculty of Engineering, Hosei University

The aim of this study was to elucidate the clinical usefulness of scatter correction with an artificial neural network (ANN) in ^{99m}Tc and ^{123}I dual-isotope SPECT. ***Methods:*** Two algorithms for ANN scatter correction were tested: ANN-10 and ANN-3 employing 10 and 3 energy windows for data acquisition, respectively. Three patients underwent myocardial or brain SPECT with one of the following combinations of radiopharmaceuticals administered: ^{99m}Tc-tetrofosmin and ^{123}I-metaiodobenzylguanidine (MIBG), ^{99m}Tc-methoxyisobutylisonitrile (MIBI) and ^{123}I-beta-methyl-paraiodophenyl-pentadecanoic acid (BMIPP), or ^{99m}Tc-ethyl-cistainate dimmer (ECD) and ^{123}I-iomazenil. The patients were also referred for single-isotope imaging incorporating conventional triple-energy window (TEW) scatter correction. Crosstalk- and scatter-corrected ^{99m}Tc- and ^{123}I-SPECT images in dual-isotope acquisition with ANN were compared with those in single-isotope acquisition. ***Results:*** The ANN method well separated ^{123}I and ^{99m}Tc primary photons. Although ANN-10 yielded images of poor quality, ANN-3 offered comparable image quality with the single-isotope scan without significant increase of acquisition time. ***Conclusion:*** The proposed method is clinically useful because it provides various combinations of information without anatomical misregistration with one acquisition.

Key words: artificial neural network, dual-isotope SPECT, scatter correction, brain SPECT, myocardial SPECT

INTRODUCTION

AN IMPORTANT FEATURE of radionuclide imaging is the capability of quantitative analysis of regional function of organs. Quantification with SPECT images is degraded by many factors such as photon scattering and attenuation, partial volume effect, collimator aperture, detector response and patient motion.[1] Regarding scatter correction, various methods have been reported, including the dual photopeak window (DPW), transmission-dependent scatter correction (TDSC) and triple energy window (TEW) methods.[2–4] Some methods are also applicable to crosstalk correction in simultaneous dual-isotope imaging.[5,6] However, it is very difficult to compensate for crosstalk between ^{99m}Tc and ^{123}I because the two radionuclides emit photons whose energies are very close to each other.

We have proposed a scatter correction method with an artificial neural network (ANN) in single-isotope imaging.[7] This method is applicable to crosstalk correction between ^{99m}Tc and ^{123}I.[8] In addition, other investigators have also reported a scatter correction method with ANN,[9] and allied it to the same dual-isotope imaging.[10,11] Furthermore, some papers discussed the clinical use of ANN in dual-isotope imaging.[12,13] However, the above mentioned methods have a common disadvantage in practicability because energy windows more than 9 are required for data acquisition; this window setting is not achievable in most commercially available SPECT systems. To overcome this problem, we have developed a scatter correction method with an ANN employing three energy windows for data acquisition.[14] This energy setting resulted in reduced image noise without impairing quantitative

Received June 19, 2006, revision accepted October 11, 2006.
For reprint contact: Jingming Bai, M.D., Department of Radiology, School of Medicine, Keio University, Tokyo 160–8582, JAPAN.
E-mail: bjingming@goo.ne.jp

accuracy in phantom experiments. In the current study, this three-window ANN method was applied to clinical myocardial and brain SPECT to elucidate its practicability and usefulness.

MATERIALS AND METHODS

Energy window setting and structure of artificial neural network

We used the following two methods to estimate the counts of primary photons ($C_{Tc\text{-}prim}$ for ^{99m}Tc and $C_{I\text{-}prim}$ for ^{123}I) after ^{99m}Tc and ^{123}I dual-isotope acquisition: an ANN with 10 inputs (ANN-10), and an ANN with 3 inputs (ANN-3).

The ANN-10 has three layers: one input layer with ten units, one hidden layer with twenty units and one output layer with two units (Fig. 1 (A)). For input values, we used ten ratios of counts determined by the two energy windows each: one was count C_k acquired with the *k*-th narrow window and the other was count C_s acquired with the broad window ranging from 120 to 180 keV. The narrow windows with a width of 6 keV were sequentially positioned in the energy range from 120 to 180 keV. The value input into the *k*-th window was the ratio R_k (= C_k/C_s). The outputs were two count ratios, $R_{I/2}$ and R_{I+Tc}. $R_{I/2}$ was the count ratio of half of the primary photons for ^{123}I to the photons measured at the upper half of the ^{123}I photo-peak window (159–180 keV) (C_{IH}). R_{I+Tc} was the count ratio of the sum of the primary photons for ^{99m}Tc and ^{123}I to the total photons C_s. With the calculated ratio $R_{I/2}$ on the basis of the neural network and the measured count C_{IH}, we estimated the primary count $C_{I\text{-}prim}$ for ^{123}I at each pixel in a planar image.

$$C_{I\text{-}prim} = 2 * C_{IH} * R_{I/2}$$

With the calculated ratio R_{I+Tc} and the measured count C_s, we calculated the primary count $C_{Tc\text{-}prim}$ for ^{99m}Tc at each pixel in the planar image.

$$C_{Tc\text{-}prim} = C_s * R_{I+Tc} - C_{I\text{-}prim}$$

In ANN-3, three energy windows (from 90 to 119 keV, from 120 to 150 keV, and from 151 to 183 keV, respectively) were set for scatter count (C_{scat}), ^{99m}Tc count (C_{Tc}) and ^{123}I count (C_I), respectively (Fig. 1 (B)). This ANN

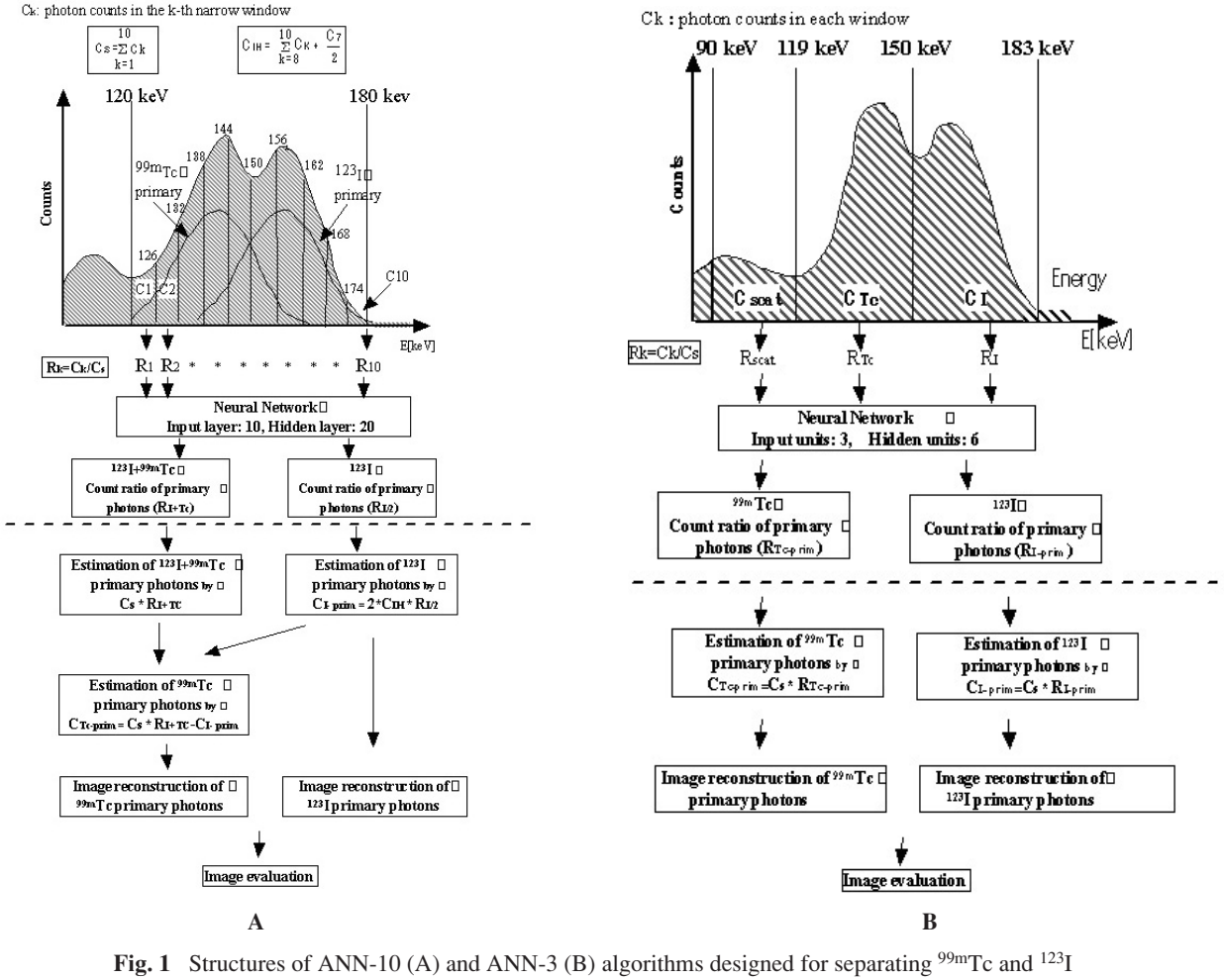

Fig. 1 Structures of ANN-10 (A) and ANN-3 (B) algorithms designed for separating ^{99m}Tc and ^{123}I primary photons in dual-isotope SPECT imaging.

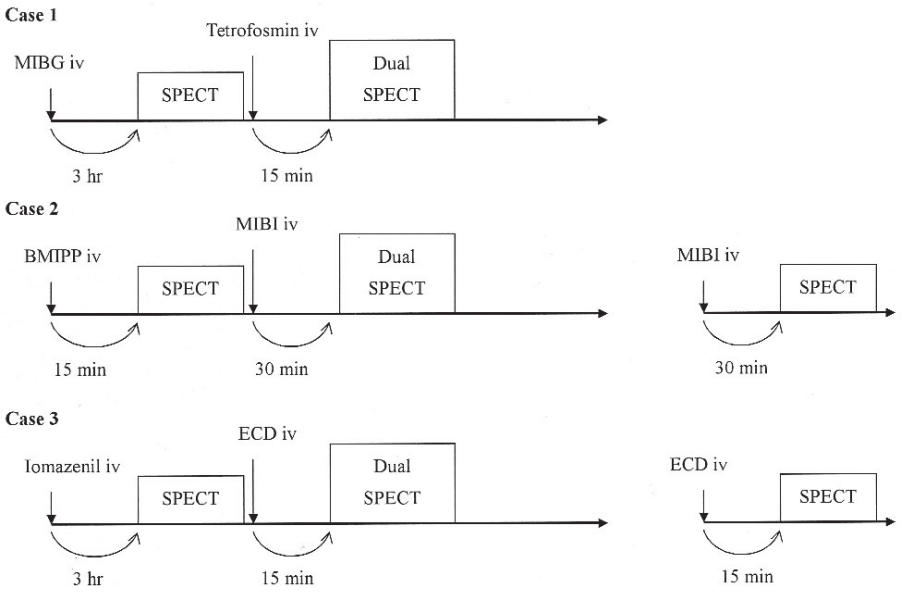

Fig. 2 Imaging protocols of the three patients.

comprises also three layers: one input layer with three units, one hidden layer with six units and one output layer with two units (Fig. 1). The inputs in the ANN-3 are three count ratios (R_{scat}, R_{Tc} and R_I) which were calculated from the above counts acquired with three energy windows and the total count (C_s) in a broad window (90–183 keV), i.e., $R_{scat} = C_{scat}/C_s$, $R_{Tc} = C_{Tc}/C_s$ and $R_I = C_I/C_s$. The output layer provides the ratios of estimated primary to total photons for ^{99m}Tc ($R_{Tc\text{-}prim}$) and ^{123}I ($R_{I\text{-}prim}$) in each pixel, respectively. The primary counts for ^{99m}Tc ($C_{Tc\text{-}prim}$) and ^{123}I ($C_{I\text{-}prim}$) at each pixel in the planar image were obtained as follows:

$$C_{Tc\text{-}prim} = C_s * R_{Tc\text{-}prim}$$
$$C_{I\text{-}prim} = C_s * R_{I\text{-}prim}$$

Both ANN-10 and ANN-3 were designed and trained with a back-propagation algorithm.[7,8,14] Several energy spectra generated by the Monte Carlo method were used as a training data set.[7,8,14]

The data were acquired simultaneously with spectrum SPECT acquisition employing 125 energy channels from 70 to 210 keV. After acquisition, the spectrum data were rearranged to 3 and 10 windows for ANN-3 and ANN-10, respectively. In ANN-10, to eliminate the scattered photons from the high energy peak (529 keV) of ^{123}I, the mean count ranging from 180 to 210 keV was subtracted from the measured total counts in each pixel. In ANN-3, as the count in the energy window from 90 to 119 keV contains the scatter fraction from the above high energy peak, no additional subtraction of photon scattering was performed.

Patients

Three patients were enrolled in the present study. Informed consent was obtained from each patient after a detailed explanation of the study. The form to obtain consent was approved by the institutional committee of Keio University Hospital.

The first patient had Parkinson's disease without a history of myocardial infarction. The patient underwent both ^{123}I-metaiodobenzylguanidine (MIBG, Daiichi Radioisotope Labs., Tokyo, Japan) and ^{99m}Tc-tetrofosmin (Nihon Medi-Physics plc. Tokyo, Japan) SPECT at rest.

The second was a patient with myocardial infarction referred for ^{123}I-beta-methyl-paraiodophenylpentadecanoic acid (BMIPP, Nihon Medi-Physics plc. Tokyo, Japan) and ^{99m}Tc-methoxyisobutylisonitrile (MIBI, Daiichi Radioisotope Labs., Tokyo, Japan) SPECT. Coronary angiography revealed stenosis in the circumflex artery.

The third was a patient with epilepsy referred for ^{123}I-iomazenil (Nihon Medi-Physics plc. Tokyo, Japan) and ^{99m}Tc-ethyl-cistainate dimmer (ECD, Daiichi Radioisotope Labs., Tokyo, Japan) SPECT.

Protocol

Imaging sequences

Figure 2 shows the examination protocols of the three patients. The first patient was injected with 111 MBq of ^{123}I-MIBG at rest and SPECT imaging was performed 3 hours after injection. Soon after the single-isotope imaging, 555 MBq of ^{99m}Tc-tetrofosmin was administered at rest followed by simultaneous ^{123}I-MIBG and ^{99m}Tc-tetrofosmin SPECT.

The second patient was injected with ^{123}I-BMIPP at rest and SPECT imaging was performed 15 minutes after injection. After completing BMIPP SPECT, ^{99m}Tc-MIBI was administered to obtain simultaneous BMIPP and MIBI SPECT. The patient also underwent MIBI SPECT

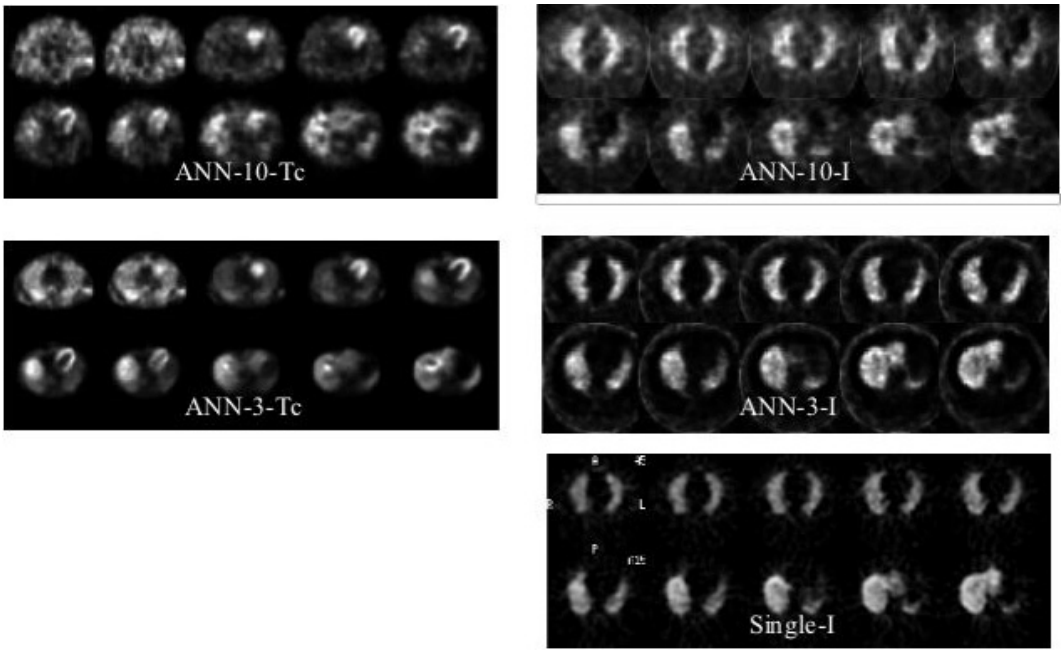

Fig. 3 Transaxial SPECT images of ^{99m}Tc-tetrofosmin and ^{123}I-MIBG in single- and dual-isotope acquisition. ANN: dual-isotope imaging using artificial neural network with 10 inputs (ANN-10) and 3 inputs (ANN-3); Tc: ^{99m}Tc-tetrofosmin; I: ^{123}I-MIBG; Single-I: single-isotope imaging with ^{123}I-MIBG.

two days after.

The last patient was injected with 222 MBq of ^{123}I-iomazenil at rest and SPECT imaging was performed 3 hours after injection. After completing iomazenil SPECT, 555 MBq of ^{99m}Tc-ECD was administered to obtain simultaneous iomazenil and ECD SPECT. The patient also underwent ECD SPECT two days after.

Instrumentation, data acquisition and image processing

A three-headed rotating gamma camera Toshiba GCA-9300A/DI with low-energy high-resolution parallel-hole collimators was used for data acquisition, and image processors DELL DIMENSION 8300 and Toshiba GMS5500U/DI were employed for image processing.

Single-isotope acquisition in each case was carried out with the TEW scatter correction method employing a 20% main photopeak window and two 7% subwindows adjacent to the main window.[3] In the projection data, the scatter fraction was estimated by the area approximation based on the counts of the subwindows, and it was removed from the counts in the main window to obtain the counts of primary photons.[3] The gamma camera rotated continuously for 16 minutes in each acquisition. SPECT data were arranged into 60 projections over 360 degrees.

In dual-isotope SPECT (ANN), 60 projections over 360 degrees (stepped by 6 degrees) were obtained. Data acquisition time for each projection angle was 50 seconds and total acquisition time was 19 minutes.

The counts of primary photons separated by the ANN-3 and ANN-10 from the acquired dual-isotope projection data were reconstructed into images of a 64 × 64 matrix using an OS-EM method with 5 iterations and 10 subsets. Attenuation correction was not conducted to either the dual-isotope or single-isotope imaging data.

Lesion-to-normal count ratios (mean count in the region-of-interest placed on the lateral wall divided by that in the septum) were obtained from the single- and dual-isotope images of the second patient undergoing ^{123}I-BMIPP and ^{99m}Tc-MIBI SPECT.

RESULTS

Figure 3 shows ^{123}I-MIBG and ^{99m}Tc-tetrofosmin transaxial SPECT images obtained with single- and dual-isotope acquisition. Dual-isotope imaging showed no cardiac uptake of ^{123}I-MIBG and well preserved uptake of ^{99m}Tc-tetrofosmin. Single-isotope imaging using ^{123}I-MIBG also manifested no cardiac uptake. Compared with ANN-10, ANN-3 offered low-noise image both in MIBG and tetrofosmin SPECT. ANN-3 provided images of comparable quality with single-isotope imaging with TEW.

Figure 4 shows ^{99m}Tc-MIBI and ^{123}I-BMIPP transaxial SPECT images. A mismatch in the lateral wall can be easily recognized between myocardial perfusion and fatty acid metabolism (preserved perfusion and impaired metabolism) in ANN-3 and single-isotope (*arrow*). In ANN-3, findings in single- and dual-isotope imaging are almost the same. On the other hand, ANN-10 failed to visualize

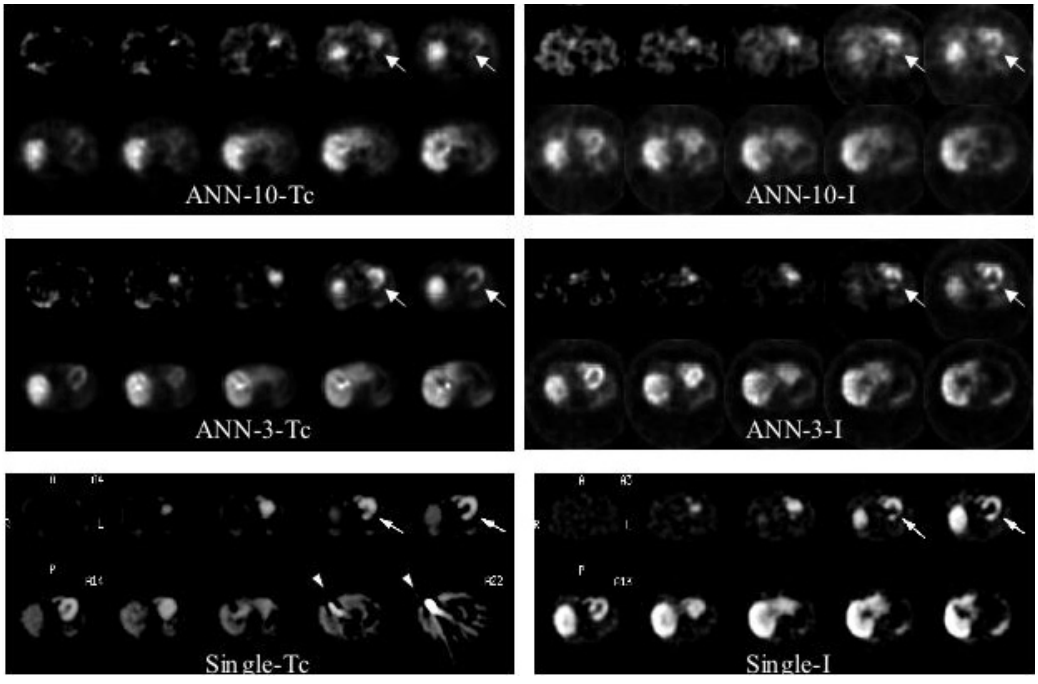

Fig. 4 Transaxial SPECT images of ^{99m}Tc-MIBI and ^{123}I-BMIPP in single- and dual-isotope acquisition. ANN: dual-isotope imaging using artificial neural network with 10 inputs (ANN-10) and 3 inputs (ANN-3); Tc: ^{99m}Tc-MIBI; I: ^{123}I-BMIPP; Single-Tc: single ^{99m}Tc-MIBI SPECT; Single-I: single ^{123}I-BMIPP SPECT; arrow: lesion site; arrowhead: biliary discharge of MIBI.

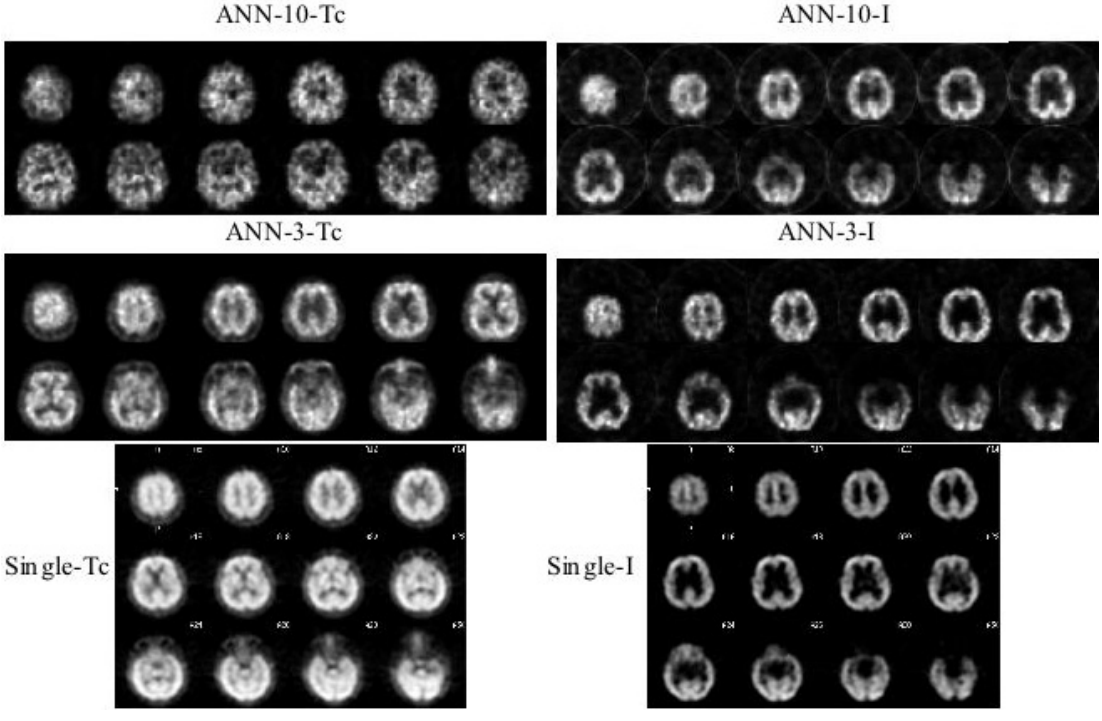

Fig. 5 Transaxial SPECT images of ^{99m}Tc-ECD and ^{123}I-iomazenil in single- and dual-isotope acquisition. ANN: dual-isotope imaging using artificial neural network with 10 inputs (ANN-10) and 3 inputs (ANN-3); Tc: ^{99m}Tc-ECD; I: ^{123}I-iomazenil; Single-Tc: single ^{99m}Tc-ECD imaging; Single-I: single ^{123}I-iomazenil imaging.

the mismatch clearly because of inferior image quality of both SPECT images. The lateral-to-septal count ratios were 0.56 and 0.46 in the single ^{99m}Tc-MIBI and single ^{123}I-BMIPP SPECT images, respectively. The count ratios were 0.63 (^{99m}Tc) and 0.46 (^{123}I) in the ANN-3 images, and 0.74 (^{99m}Tc) and 0.60 (^{123}I) in the ANN-10 images.

Figure 5 includes ^{123}I-iomazenil and ^{99m}Tc-ECD transaxial SPECT images. In dual-isotope imaging with ANN-3, both ^{123}I-iomazenil and ^{99m}Tc-ECD SPECT showed normal uptake in the cerebral cortex. On the other hand, marked differences in the uptake were observed in the basal ganglia and thalamus: preserved uptake in ^{99m}Tc-ECD SPECT and almost no uptake in ^{123}I-iomazenil SPECT. Compared with ANN-3, ANN-10 yielded inferior image quality especially in ^{99m}Tc-ECD transaxial SPECT. Although image quality in the basal ganglia and thalamus in ECD SPECT of ANN-3 is inferior to that of single-I-123 imaging, visualization of the cerebral cortex is of acceptable quality in ANN-3.

DISCUSSION

Dual-isotope imaging has two main advantages. The first is that it provides two different kinds of information with one scan and accordingly reduces examination time and burden to patients and medical staff. The second is that there is no problem of anatomical misregistration between the two images. In contrast, the crosstalk hampers the use of two radionuclides whose photon energies are close to each other. Thus, most clinical SPECT protocols employ the combination of ^{201}Tl and ^{99m}Tc, or ^{201}Tl and ^{123}I. Since ^{201}Tl cannot be used to label compounds, information obtained from it is limited to myocardial perfusion or tumor cell viability. On the other hand, ^{99m}Tc and ^{123}I are available for labeling various compounds, and dual-isotope imaging with ^{99m}Tc and ^{123}I engenders a vast array of information. Therefore, we contrived a scatter correction method (ANN) enabling ^{99m}Tc and ^{123}I dual-isotope acquisition and applied it to myocardial and brain SPECT.

When we first developed a scatter correction method with ANN (ANN-10 in the present study), it was used to compensate for scattered photons in ^{99m}Tc single-isotope acquisition.[7] However, other easier methods such as TEW can eliminate scattered photons in single-isotope acquisition or dual-isotope acquisition with ^{201}Tl and ^{99m}Tc, or ^{201}Tl and ^{123}I.[2–4] On the other hand, a distinguishing feature of the method with ANN is its applicability in ^{99m}Tc and ^{123}I dual-isotope imaging.[8,14] Since a series of simulation and phantom experiments showed its acceptable image quality and quantitative accuracy,[7,8,14] clinical myocardial and brain SPECT imaging was conducted in the present study. We compared the performance of the original method (ANN-10) and its revised version (ANN-3).

Regarding the difference between ANN-10 and ANN-3, ANN-3 has some advantages compared with its counterparts. First, the reduced number of energy windows in ANN-3 results in a reduced amount of acquired data and shortened time for data processing. Second, increasing the widths of energy windows offers easy uniformity maintenance of the camera system and increased signal-to-noise ratios leading to improved image quality. The images obtained in the three cases clearly reveal the difference in image quality between ANN-3 and ANN-10. Third, improved accuracy in quantifying myocardial uptake can be expected. Quantitative analysis of the severity of the infarcted myocardium in the second case shows the superiority of ANN-3 over ANN-10. Finally, routine clinical application of ANN-10 cannot be expected yet because commercially available SPECT cameras do not fit the setting of so many energy windows. Therefore, ANN-3 has considerable superiority over ANN-10 in clinical practice.

In comparing ANN-3 and single-isotope acquisition, acquisition time of dual-isotope imaging is comparable (19 minutes for ANN-3 and 16 minutes for single acquisition) and image quality obtained by ANN-3 is also acceptable. Therefore, ANN-3 has clinical feasibility for dual-isotope imaging.

The first patient underwent simultaneous ^{123}I-MIBG and ^{99m}Tc-tetrofosmin SPECT. The patient contracted Parkinson's disease without a history of cardiac disease, and it is well known that patients with Parkinson's disease often manifest no cardiac uptake or severely reduced uptake of MIBG despite the absence of cardiac disease like this case.[15,16] In such cases, concurrent myocardial perfusion imaging is useful to judge whether this reduced uptake is caused by Parkinson's disease itself or cardiac disease. Simultaneous acquisition reduces the burden to patients especially when the patient suffers from parkinsonism making it difficult to keep still for a long time during data acquisition.

The second patient was referred for simultaneous ^{123}I-BMIPP and ^{99m}Tc-MIBI SPECT. The discrepancy between BMIPP and perfusion images (so-called perfusion-metabolism mismatch) in patients with unstable angina or myocardial infarction suggests the metabolic switch from fatty acid metabolism to glycolysis in the myocardium.[17,18] It is reported that assessing this mismatch is of clinical value because it is related to reversibility of impaired cardiac function and the occurrence of cardiac events.[19] By using ^{99m}Tc instead of ^{201}Tl, it would be easier to estimate the metabolism-perfusion mismatch, because ^{99m}Tc is less susceptible to photon attenuation and allows images of excellent quality.

Dual-isotope brain SPECT with ^{123}I-iomazenil and ^{99m}Tc-ECD was performed on the third patient suspected of having epilepsy. Iodine-123-iomazenil is a benzodiazepine receptor imaging agent and the benzodiazepine receptor density decreases in epileptic foci.[20,21] It has

been confirmed that the distribution of benzodiazepine receptors is ubiquitous in cerebral cortex and that the receptor density is very low in basal ganglia and thalamus.[22,23] The images obtained in this patient are compatible with the above fact. Although SPECT did not reveal the epileptic focus in this patient, the dual-isotope imaging with ^{123}I-iomazenil and ^{99m}Tc-ECD may be useful in diagnosing and treating patients with epilepsy because it provides information about the cause of receptor loss (associated cerebral infarction and so on). In addition, when using this protocol in patients with cerebrovascular disease, it would reveal the accurate sites of ischemic penumbra because of the lack of no anatomical misregistration.[24,25]

The crosstalk between two radionuclides in dual-isotope imaging depends on the ratio of the administered doses. In the present study, we injected 111 MBq or 222 MBq of ^{123}I and 555 MBq of ^{99m}Tc, which are standard doses used in the clinical setting. However, further study is needed to elucidate the feasibility of ANN under extraordinary combinations of injected doses for employing newly developed radiopharmaceuticals or imaging protocols.

CONCLUSION

We applied scatter correction with an artificial neural network to ^{123}I and ^{99m}Tc dual-isotope SPECT in clinical myocardial and brain imaging. The correction method (ANN-3) well separated ^{123}I and ^{99m}Tc primary photons and yielded images of acceptable quality without a significant increase of the acquisition time. The proposed method provides various combinations of information through simultaneous acquisition of ^{123}I and ^{99m}Tc, both of which can label various compounds.

ACKNOWLEDGMENTS

This research is partially supported by the Ministry of Education, Culture, Sports, Science and Technology, Grant-in-Aid for the 21st Century Center of Excellence (COE) Program entitled "Basic study and clinical application of human stem cell biology and immunology: Approaches based on the development of experimental animal models" (Keio University). This study is also partially supported by Grant-in-Aid for Scientific Research (15591302 and 18790912) from the Ministry of Education, Culture, Sports, Science and Technology.

REFERENCES

1. Ogawa K. Image distortion and correction in single photon emission CT. *Ann Nucl Med* 2004; 18: 171–185.
2. King MA, Hademenos GJ, Glick SJ. A dual-photonpeak window method for scatter correction. *J Nucl Med* 1992; 33: 605–612.
3. Ogawa K, Harata Y, Ichihara T, Kubo A, Hashimoto S. A practical method for position-dependent Compton-scatter correction in single photon emission CT. *IEEE Trans Med Imag* 1993; 10: 408–412.
4. Meikle SR, Hutton BF, Bailey DL. A transmission-dependent method for scatter correction in SPECT. *J Nucl Med* 1994; 35: 360–367.
5. Ichihara T, Ogawa K, Motomura N, Kubo A, Hashimoto S. Compton scatter compensation using the triple-energy window method for single- and dual-isotope SPECT. *J Nucl Med* 1993; 34: 2216–2221.
6. Tsuji A, Kojima A, Matsumoto M, Oyama Y, Tomiguchi S, Kira T, et al. A new method for crosstalk correction in simultaneous dual-isotope myocardial imaging with Tl-201 and I-123. *Ann Nucl Med* 1999; 13: 317–323.
7. Ogawa K, Nishizaki N. Accurate scatter compensation using neural networks in radionuclide imaging. *IEEE Trans Nucl Sci* 1993; 40: 1020–1025.
8. Ishii M, Ogawa K, Nakahara T, Hashimoto J, Kubo A. Quantification of ^{123}I and ^{99m}Tc in dual-isotope SPECT with an artificial neural network. *Med Imag Tech* 2004; 22: 155–163.
9. Maksud P, Fertil B, Rica C, Fakhri GE, Aurengo A. Artificial neural network as a tool to compensate for scatter and attenuation in radionuclide imaging. *J Nucl Med* 1998; 39: 735–745.
10. Fakhri GE, Maksud P, Kijewski MF, Haber MO, Todd-Pokropek A, Aurengo A, et al. Scatter and cross-talk corrections in simultaneous ^{99m}Tc/^{123}I brain SPECT using constrained factor analysis and artificial neural networks. *IEEE Trans Nucl Sci* 2000; 47: 1573–1580.
11. Fakhri GE, Moore SC, Maksud P, Aurengo A, Fijewski MF. Absolute activity quantitation in simultaneous ^{123}I/^{99m}Tc Brain SPECT. *J Nucl Med* 2001; 42: 300–308.
12. Zheng XM, Zubal IG, Seibyl JP, King MA. Correction for scatter and cross-talk contamination in dual radionuclide Tc-99m and I-123 images using an artificial neural network. *IEEE Trans Nucl Sci* 2004; 51: 2649–2653.
13. El Fakhri G, Habert MO, Maksud P, Kas A, Malek Z, Kijewski MF, et al. Quantitative simultaneous (^{99m})Tc-ECD/^{123}I-FP-CIT SPECT in Parkinson's disease and multiple system atrophy. *Eur J Nucl Med Imaging* 2006; 33: 87–92.
14. Ogawa K, Suzawa K. Quantification of two radionuclides in simultaneous ^{123}I/^{99m}Tc SPECT with artificial neural networks. *IEEE Nuclear Science Symposium and Medical Imaging Conference* 2004; 6: 3689–3693.
15. Satoh A, Serita T, Seto M, Tomita I, Satoh H, Iwanaga K, et al. Loss of ^{123}I-MIBG uptake by the heart in Parkinson's Disease: Assessment of cardiac sympathetic denervation and diagnostic value. *J Nucl Med* 1999; 40: 371–375.
16. Orimo S, Amino T, Ozawa E, Kojo T, Uchihara T, Takahashi A, et al. A useful marker for differential diagnosis of Parkinson's disease—MIBG myocardial scintigraphy. *Rinsho Shinkeigaku* 2004; 44: 827–829.
17. Opie LH, Owen P, Riemersma RA. Relative rates of glucose and free fatty acids by ischemic and nonischemic myocardium after coronary artery ligation in the dog. *Eur J Clin Invest* 1973; 3: 419–435.
18. Tadamura E, Tamaki N, Kudoh T, Hattori N, Konishi J. BMIPP compared with PET metabolism. *Int J Card Imaging* 1999; 15: 61–69.
19. Taki J, Nakajima K, Matsunari I, Bunko H, Takata S,

Kawasuji M, et al. Assessment of improvement of myocardial fatty acid uptake and function after revascularization using iodine-123-BMIPP. *J Nucl Med* 1997; 38: 1503–1510.
20. Savic I, Widen L, Thorell JO, Blomqvist G, Ericson K, Roland P. Cortical benzodiazepine receptor binding in patients with generalized and partial epilepsy. *Epilepsia* 1990; 31: 724–730.
21. Savic I, Pauli S, Thorell JO, Blomqvist G. *In vivo* demonstration of altered benzodiazepine receptor density in patients with generalized epilepsy. *J Neurol Neurosurg Psychiatry* 1994; 57: 797–804.
22. Shinotoh H, Yamasaki T, Inoue O, Itoh T, Suzuki K, Hashimoto K, et al. Visualization of specific binding sites of benzodiazepam in human brain. *J Nucl Med* 1986; 27: 1593–1599.
23. Woods SW, Seibyl JB, Goddard AW, Dey HM, Zoghbi SS, Germine M, et al. Dynamic SPECT imaging after injection of the benzodiazepine receptor ligand [^{123}I]iomazenil in healthy human subjects. *Psychiatry Res* 1992; 45: 67–77.
24. Hatazawa J, Satoh T, Shimosegawa E, Okudera T, Inugami A, Ogawa T, et al. Evaluation of cerebral infarction with iodine 123-iomazenil SPECT. *J Nucl Med* 1995; 36: 2154–2161.
25. Hashimoto J, Sasaki T, Itoh Y, Nakamura K, Kubo A, Amano T, et al. Brain SPECT imaging using three different tracers in subacute cerebral infarction. *Clin Nucl Med* 1998; 23: 275–277.